STRENGTH OF WOOD BEAMS WITH FILLETED INTERIOR NOTCHES: A NEW MODEL

Barry L. Zalph

Consultant
Technical Articulation
P.O. Box 484, Blacksburg, VA 24063-0484

and

Thomas E. McLain

Professor
Department of Wood Science and Forest Products
Virginia Polytechnic Institute and State University
Blacksburg, VA 24061-0503

(Received May 1991)

ABSTRACT

A critical fillet hoop stress (CFHS) model has been used to develop an expression for predicting the failure loads of beams with notches on the tension side between the supports. The effects of notch location and loading condition are described well by a single parameter, V/M, the ratio of resultant shear to resultant moment at the section containing the critical notch fillet. Effects of notch depth, fillet radius, and beam depth are treated explicitly in the model. Computer modeling and mechanical testing showed negligible effects of notch length and beam span. The model has been verified with notched beam tests of eight wood materials, three notch locations, and twenty-one filleted notch geometries. The closed-form strength equation, with a single material parameter (κ), accurately described the observed trends in experimental notched beam critical loads with respect to notch and beam geometry, notch location, and loading geometry.

Keywords: Beam, fillet, finite element modeling, notch, strength measurement, strength prediction.

INTRODUCTION

Notches on the tension face generally cause a major reduction in the bending strength of wood beams (Stieda 1966; Gerhardt 1984a). Interior notches (i.e., located between the supports) are found in roof rafters and floor joists used in building construction (Anderson 1975), either by design or by on-site modification. The most common planned use of notched beams, however, is in wood pallet stringers. Over 300 million notched wood stringer pallets were made in the United States in 1989, nearly all of which used notches with filleted (rounded) corners (Stern 1990). Accurate estimates of the load capacity and reliability of these structures require accurate estimates of the strength-reducing effect of tension face interior notches.

The complexities of the stress distributions around notches, combined with difficulties in defining and measuring material properties governing notched beam fracture, have hindered the development of an accurate, general method for estimating the capacity of notched wood beams. Previous investigations have calculated stresses or stress intensity factors in notched orthotropic bodies and used a combined-stress or mixed-mode failure criterion to predict the onset of cracking. Classical stress-based computations and experiments have been conducted by Green (1942), Green and Taylor (1945), Stieda (1964, 1966), and Abou-Ghaida and Gopu (1984). Numerous workers have employed linear elastic fracture mechanics (LEFM) to analyze notched beams (e.g., Porter 1964; Leicester and Poynter 1979; Mur-

Wood and Fiber Science, 24(2), 1992, pp. 204–215

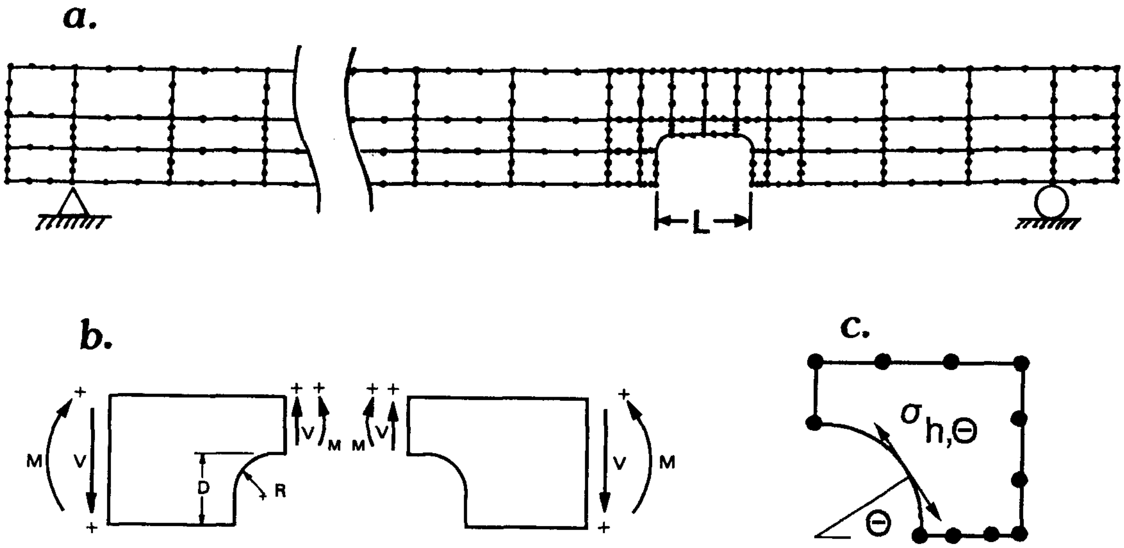

FIG. 1. a) FE mesh for off-center-notched beam. D = 1.75 in., R = 0.75 in., L = 3 in., h = 3.5 in. b) Sign convention for resultant moment (M) and shear (V). Positive moment and shear give rise to tensile fillet hoop stress, σ_h. c) Hybrid fillet element, showing direction of fillet hoop stress, $\sigma_{h,\theta}$, at fillet angle θ.

phy 1979, 1986; Mall et al. 1983; Gustafsson 1988). Although LEFM theory is well developed for sharp-cornered notches, its practical application is impeded by the difficulty of obtaining reliable measurements of the necessary fracture toughnesses and elastic parameters.

Design guidance for interior-notched beams is quite limited. The *Wood Handbook* (USDA 1987) gives an equation, based on the analysis of Murphy (1979), that predicts crack initiation loads for sharp-cornered notches under combined shear and moment. The material parameters are fixed at values "... conservative for most species." Since it neglects material-dependent strength differences and the benefits of rounding notch corners (Gerhardt 1984a), that equation is likely to be overconservative in many cases. Tension face interior notches are also within the purview of the Australian Timber Engineering Code AS 1720.1-1988 (Standards Assoc. of Australia 1988). Like Murphy's equation, the Australian method was derived using LEFM and treats only sharp-cornered notches. Notch depth has essentially no influence on the calculation except for its effect on nominal net section stresses. This is at odds with Gerhardt's (1984a) finding that stress concentrations are strongly related to notch depth.

In a study of notch geometries of importance for pallet stringers, Gerhardt (1984a) found that the moment capacity of notched green red oak beams could be predicted from a simple equation involving notch depth and a single material parameter. His finite element (FE) analysis used a hybrid plane stress orthotropic element to model the fillet region (Gerhardt 1984b). This element computes fillet hoop stress (σ_h), i.e., the stress tangent to the free surface of the rounded notch corner (Fig. 1). Maximum fillet hoop stress ($\sigma_{h,max}$) was found to occur within a small range of angles along the fillet for all of the 252 beams modeled. This indicates a fairly consistent ratio of longitudinal to transverse tensile stresses at the location of $\sigma_{h,max}$. From his FE results, Gerhardt derived a closed-form expression for calculating $\sigma_{h,max}$. The functional relationship between maximum hoop stress and notch depth, which was independent of assumed elastic properties, was found to fit the experimental failure data very well. This implies that fracture initiates at a critical value of σ_h. This observation allowed failure predictions to be made without resorting to a combined stress failure criterion.

Starting from Gerhardt's critical fillet hoop stress (CFHS) hypothesis, we: 1) verified the applicability of the CFHS hypothesis to a wide variety of wood materials; 2) developed a model to include the effects of fillet radius, notch length, beam depth, and beam span in addition to notch depth and loading conditions; 3) established relationships between notched beam strength and readily available wood property data; and 4) tested extensions of the model to treat sharp-cornered notches. This paper describes the first three phases of the work.

PROJECT OVERVIEW

Finite element modeling was performed to calculate maximum fillet hoop stress, $\sigma_{h,max}$, in 879 beams with interior notches on the tension face. Relationships were sought between $\sigma_{h,max}$ and notch geometry (depth, fillet radius, length), loading condition, elastic parameters, and beam depth and span. These relationships were used to derive a closed-form expression to approximate $\sigma_{h,max}$ from the geometric inputs and a single material parameter. This expression was rearranged to allow its application to notched beam test data. Tests of 837 notched beams were used to evaluate the material parameter for eight wood materials and to verify the geometry dependencies predicted by the closed-form expression. Regression relationships were established between the notched beam strength parameter and standard wood properties. Strength predictions from the resulting model were compared with those of previous models. Details of the experimental designs, procedures, and results are described by Zalph (1989).

FINITE ELEMENT MODELING

The finite element (FE) method was used to calculate stresses, strains, and displacements in notched beams. The analyses employed the FE program developed by Gerhardt (1984a) using a single hybrid fillet element (Gerhardt 1984b) at each notch fillet and cubic isoparametric displacement-based elements (Gerhardt 1983) elsewhere in the mesh. All input data were prepared by a mesh generator program (Zalph 1989). A typical mesh is shown in Fig. 1a.

Plane stress conditions were assumed. An orthotropic, linear-elastic formulation was used with material axes coinciding with the beam axes (i.e., no slope of grain). The hybrid fillet element satisfies all governing differential equations of anisotropic elasticity within the element and models exactly the shape and stress-free condition of the circular fillet surface. This obviates the need for a fine element mesh in the region of the discontinuity.

We performed three sets of FE calculations. The main study considered the effects of notch geometry, notch location, loading condition, and elastic parameters on maximum fillet hoop stress, $\sigma_{h,max}$, at a constant beam depth, h = 3.5 in. The two substudies focused on the effect of beam depth over the range 3.5 in. $\leq$ h $\leq$ 10.5 in. The FE investigations were designed to test the generality of Gerhardt's formulation (1984a) and to facilitate the derivation of algebraic equations to approximate the effects of the independent variables on $\sigma_{h,max}$. All notches studied were rectangular with rounded corners, i.e., each notch fillet was a 90° arc (Fig. 1). Notches were characterized by their depth, D, length, L, and fillet radius, R. All notches had D $\geq$ R and L $\geq$ 2R; the limiting case of D = R and L = 2R describes a semicircular notch.

The main FE study included 675 computations of $\sigma_{h,max}$. The fifteen notch geometries included 0.5 in. $\leq$ D $\leq$ 2.5 in., 0.2 in. $\leq$ R $\leq$ 0.5 in., and 1 in. $\leq$ L $\leq$ 9 in., as shown in Table 1. The levels of D, R, and L were chosen according to a central composite design (CCD) (Myers 1971). The CCD allows a sample space with several independent variables to be probed efficiently when terms up to second order may be present and the levels of the independent variables can be precisely controlled by the experimenter. Five orthotropic property sets, shown in Table 2, were used to cover the range of common wood properties. The orthotropy

TABLE 1. *Notch geometries in main FE study.*

D, in.	R, in.	L, in.
0.5000	0.35000	5.0000
0.9060	0.26091	7.3758
0.9060	0.26091	2.6242
0.9060	0.43909	7.3758
0.9060	0.43909	2.6242
1.5000	0.20000	5.0000
1.5000	0.35000	9.0000
1.5000	0.35000	5.0000
1.5000	0.35000	1.0000
1.5000	0.50000	5.0000
2.0940	0.26091	7.3758
2.0940	0.26091	2.6242
2.0940	0.43909	7.3758
2.0940	0.43909	2.6242
2.5000	0.35000	5.0000

ratios E_x/G_{xy} and E_x/E_y influence the maximum hoop stress by affecting the ratios of longitudinal to transverse tensile stress and tensile to shear stress (Gerhardt 1984a). Poisson's ratio, ν_{xy}, was set to 0.40 in all cases as this parameter was found to exert minimal influence on the computed results (Gerhardt 1984a). For each notch geometry, three notch locations (centered and with the top of the inside fillet 10 in. and 20 in. from the nearest support) and three loading conditions (center-point, quarter-point, and uniformly distributed loads) were used.

Finite element substudy A involved beam depth and span in addition to notch geometry, loading type, and material properties. It used the G32-E12 elastic parameter (EP) set with independent variables $\phi \equiv D/h$, R, L, h, and span, s. Finite element substudy B used the G8-E12 EP set with independent variables ϕ, R, L, and h. (Span was dropped from substudy B as it had no impact in substudy A. See "Results and Discussion.") Dimensionless notch depth, ϕ, was substituted for D to allow more straightforward interpretation of any beam depth effect. Forty-three notch geometries were included in substudy A and 25 in substudy B.

For substudies A and B, a single off-center notch geometry was used with the three loading conditions described above. This resulted in three $\sigma_{h,max}$ values for each beam. Levels of R were similar to those in the main study. Beam depths of 3.5–10.5 in. were used in both substudies. Substudy A also included span over the range 44–88 in. A fixed span of 44 in. was used in substudy B.

Formulation of a closed-form expression

The critical fillet hoop stress hypothesis is that notched beams crack when $\sigma_{h,max}$ exceeds a critical value. The purpose of the closed-form expression is to estimate $\sigma_{h,max}$ without resorting to the FE model. Gerhardt (1984a) found that:

$$\sigma_{h,max} \cong f_1 \cdot \left(\frac{6M}{th^2}\right) + f_2 \cdot \left(\frac{6V}{th}\right) \qquad (1)$$

where:

f_1 = dimensionless apparent stress concentration factor for resultant moment;
f_2 = dimensionless apparent stress concentration factor for resultant shear;
M = resultant moment at the cross section containing the top of the critical fillet;
V = resultant shear at the cross section containing the top of the critical fillet.

It was helpful to rearrange Eq. (1) into the form:

TABLE 2. *Elastic parameter (EP) sets for FE computations.*

Designation	E_x 10^6 psi	E_y 10^6 psi	G_{xy} 10^6 psi	ν_{xy}	E_x/E_y	E_x/G_{xy}
G8-E12	1.2	0.100	0.1500	0.40	12	8
G12-E12	1.2	0.100	0.1000	0.40	12	12
G17-E17	1.7	0.100	0.1000	0.40	17	17
G22-E22	1.1	0.050	0.0500	0.40	22	22
G32-E12	1.2	0.100	0.0375	0.40	12	32

$$\mathrm{MCF} \equiv \frac{\sigma_{h,max}}{\left(\frac{6M}{th^2}\right)} = f_1 + f_2 \cdot \left(\frac{V}{M}\right) \cdot h \qquad (2)$$

"Moment Concentration Factor" (MCF) is the maximum hoop stress normalized by the nominal bending stress in an unnotched beam of the same gross section, at the location of the critical section. For the shear-free case, Eq. (2) reduces to MCF = f_1. The quantity (V/M) relates to loading condition and notch location; it is easily calculated from shear and moment diagrams (Byars and Snyder 1975). For a notch in a shear-free region, e.g., between quarter-point loads, V/M = 0. For beams in center-point bending with notches away from midspan, the notch fillet under higher moment is also under positive shear (Fig. 1b), while the fillet experiencing lower moment is under negative shear. The sign convention for moment and shear, originated by Gerhardt (1984a), assigns the positive sense to forces resulting in tensile fillet hoop stress, σ_h. The fillet closer to midspan has V/M > 0 and experiences higher $\sigma_{h,max}$, whereas the fillet closer to the support has V/M < 0 and experiences lower $\sigma_{h,max}$. Thus, the fillet closer to midspan is the critical fillet. For this loading condition, the top of the critical fillet is located 1/(V/M) from the nearest support.

The stress concentration factors f_1 and f_2 in Eq. (1) are functions of notch geometry and elastic parameters. For engineering use, it is helpful to separate the geometry dependence from the material dependence. A simple approach is to assume material constants, μ_M and μ_V, and material-independent stress concentration factors, F_1 and F_2, such that:

$$f_1 = \mu_M F_1 \quad \text{and} \quad f_2 = \mu_V F_2 \qquad (3)$$

Then, Eq. (1) can be rewritten:

$$\frac{6M}{th^2} = \frac{\sigma_{h,max}}{\mu_M F_1 + \mu_V F_2 \cdot h \cdot \frac{V}{M}}. \qquad (4)$$

Unfortunately, this does not allow algebraic separation of the material-dependent terms ($\sigma_{h,max}$, μ_M, μ_V) from the geometric terms (F_1, F_2, h, V/M). If $\mu_M = \mu_V = \mu$, then:

$$\frac{6M}{th^2} = \frac{\sigma_{h,max}}{\mu} \cdot \frac{1}{F_1 + F_2 \cdot h \cdot \frac{V}{M}} \qquad (5)$$

The validity of this simplification is discussed in "Results and Discussion: Finite Element Modeling" below.

The CFHS hypothesis is that cracking occurs when $\sigma_{h,max} \geq \sigma_{h,i}$, where $\sigma_{h,i}$, the fillet hoop stress at crack initiation, is a material parameter. Defining $\kappa_i \equiv \sigma_{h,i}/\mu$ allows Eq. (5) to be rewritten:

$$\frac{6M_i}{th^2} = \frac{\kappa_i}{F_1 + F_2 \cdot h \cdot \frac{V}{M}} \qquad (6)$$

where:

M_i ≡ resultant moment at the critical fillet at crack initiation; and

κ_i ≡ notched beam strength parameter for crack initiation.

κ_i is the only material-dependent term and, as such, κ_i should be independent of notch, beam, and loading geometry. Equation (6) predicts notched beam capacity. Functions F_1 and F_2, once determined, reduce to known constants for a given notch geometry. The ratio V/M is known for any given loading geometry.

MECHANICAL AND PHYSICAL TESTING

The experimental work served four primary purposes: 1) to test the validity of the CFHS model for a variety of notched beams; 2) to evaluate the material constant, κ; 3) to find a relationship between κ and other wood properties; and 4) to estimate the variability of notched beam strength. Satisfying these objectives involved tests of notched and unnotched beams and small, clear specimens of several wood materials.

Notched beam tests

The notched beam tests were performed in three studies, denoted 1, 2, and 3 in chronological order. Study 1 provided an initial assessment of the theoretical model applied to materials other than green red oak, the only material tested by Gerhardt (1984a). Results were used to select the ranges of R and L explored in the subsequent studies. Study 2 was the principal effort (771 beams) to validate the theoretical model for eight wood materials. Study 3, discussed elsewhere (Zalph 1989), explored extensions to the model to handle sharp-cornered notches and very short notches (i.e., slit notches).

Study 1 was a full factorial experiment with two levels each of D and L and 3 levels of R. Two levels of D were included to check for interactions between D and R or L. Three levels of R (0, 0.25, and 0.375 inch) were used to probe the transition from filleted to unfilleted notch behavior (Zalph 1989). L $\approx$ 0.75 in. and L $\approx$ 9.0 in., and D $\approx$ 0.6 in. ($\phi \approx 0.17$) and D $\approx$ 2.0 in. ($\phi \approx 0.57$), were chosen as reasonable extremes.

Dry (MC $\approx$ 9%) red oak and dry true fir (*Abies* spp.) were used to represent very different anatomical and mechanical properties. One loading case, V/M = 0 (pure bending throughout the notch region), was used to evaluate κ and allow preliminary verification of F_1. Generally, two beams were tested per cell.

In study 2, quarter-point and center-point bending tests were conducted using 3 notch locations, 15 notch geometries, and 8 different wood materials. (Green and kiln-dried groups of the same species were treated as separate materials. See Table 3.) Notch location and loading geometry were treated through the ratio V/M. Quarter-point loading of center-notched beams gave V/M = 0. Center-point loading of beams notched off center provided V/M ratios of 0.05 in.$^{-1}$ and 0.10 in.$^{-1}$, as in the FE modeling.

Notch length was fixed at 1.5 in. as study 1 showed no significant effect of L over the range 1–9 in. This finding was supported by the FE results reported below. Average moisture content (MC) for all green beams exceeded 29%. The MC for each dry material group was about 10%, with little variation; the exception was the red oak with MC of 5–6%. (The red oak of study 2 was from a different source and dried differently than that of study 1.) The test materials span the ranges of density, anatomical structure, and moisture content representative of commercial North American woods.

TABLE 3. *Experimental design—main notched beam study (2).*

	Levels[a]
Beam dimensions, in.: h $\approx$ 3.5, t $\approx$ 1.5, s $\approx$ 44	(1)
Notch dimensions:	
Notch depth, D, in.: 0.75, 1.1, 1.45, 1.8, 2.15	(5)
Fillet radius, R, in.: 0.25, 0.5, 0.75	(3)
V/M, in.$^{-1}$: 0, 0.05, 0.10	(3)
Material: Douglas-fir, dry; southern yellow pine, dry and green; spruce, dry; hard maple, green; red oak, dry; yellow-poplar, dry and green	(8)
Replications: 2 per cell, plus a third "center run" (D $\approx$ 1.45 in., R $\approx$ 0.5 in.), i.e., *31* tests per level of V/M for each material.	
Total tests: 31 × 3 × 8 = 744, + 24 additional for SYP sub-study, +3 extra replications = *771.*	

[a] Number of levels of the given factor.

All filleted notches were machined using a router and custom templates. All notches were essentially smooth in the corner region that governs crack initiation. Bending tests were performed at a fixed crosshead rate of 0.10 in./min. A deflection yoke equipped with a linear variable differential transformer (LVDT) was used to measure transverse deflection at midspan. Applied deflection and corresponding load were continuously recorded. The notch region was visually observed for crack initiation, which commonly coincided with an identifiable event on the load-deflection trace.

Clear wood tests

Small, clear specimens were cut from each broken beam for measurements of moisture content (MC) and dry-basis density (G). Additional specimens were taken from one third of the beams ($\geq$30 of each material) for determination of shear and perpendicular-to-grain tensile strengths (S and $T_{\perp}$, respectively) using the procedures of ASTM D-143 (Amer. Soc. for Testing and Materials 1986). Specimen thickness was limited to the beam thickness of about 1.5 in., rather than the ASTM specification of 2.0 in. The differences due to this change in specimen thickness have been shown to be small (Bendtsen and Porter 1978; Barrett 1974). Thirty unnotched beams matched to each material group were loaded in quarter-point bending to establish modulus of elasticity (MOE) and modulus of rupture (MOR) values for each group.

RESULTS AND DISCUSSION

Finite element modeling

Equation (2) posits a linear relationship between normalized maximum fillet hoop stress (MCF) and V/M. Linear regressions of MCF versus (h·V/M) were used to evaluate f_1 and f_2 for each combination of notch geometry and elastic parameters in the three FE studies. All 75 regressions from the main study (h = 3.5 in.) were very highly significant ($P \leq 0.0001$) with coefficients of determination $r^2 \geq 0.93$; in 56 of 75 cases (75%), $r^2 \geq 0.98$. All regressions in substudies A and B yielded $r^2 \geq 0.96$, and in 57 of the 68 cases (84%), $r^2 \geq 0.99$. This validates the decomposition of fillet hoop stress into a shear-related term and a moment-related term. These results suggest that the effects of notch location and loading condition are fully described by a single term, V/M, as suggested by Eqs. (2) and (4)–(6).

The angular location (θ_{max}) of $\sigma_{h,max}$ along the critical fillet is important for two reasons. First, it can be compared with experimental observations as a rough test of the hypothesis that cracking initiates at the point of maximum fillet hoop stress. Second, it is unlikely that a single critical hoop stress value would characterize failure of notched beams of a given material if θ_{max} varied widely from case to case, because large variations in θ_{max} would imply widely different combinations of longitudinal and transverse stresses at the critical section. For all notches modeled, θ_{max} was 1.5°–8° from the notch root. This is consistent with the findings of Gerhardt (1984a). Our notched beam tests generally confirmed that cracking initiates slightly away from the notch root.

The influence of elastic parameters on MCF was evaluated from the results of the main study using Eqs. (3)–(5). F_1 and F_2 are hypothesized to be material-invariant functions of notch and beam geometry, and the material parameter μ should be independent of geometry. We set $\mu = 1$ for the G17-E17 EP set, making this the baseline against which the effect of elastic properties was calibrated. For the G17-E17 results, F_1 and F_2 are equivalent to f_1 and f_2. From the regressions described above, f_1 and f_2 were calculated for each of the 75 combinations of notch geometry and elastic parameters. The proposed material parameter μ was derived for each EP set using two separate linear regressions; one allowed a nonzero intercept while the other did not:

$$MCF_k = a + b \cdot MCF_{baseline} \qquad (7)$$

$$MCF_k = \mu_k \cdot MCF_{baseline} \qquad (8)$$

where subscript k indicates the kth EP set.

Equation (7) always gave a nonsignificant intercept, i.e., a = 0. All regressions were unquestionably significant ($P \ll 0.0001$) and the resulting values of μ are given in Table 4. Several features are noteworthy. The low standard error of μ, across levels of V/M and notch geometry, is striking. This supports the validity of the one-constant formulation of Eq. (5). The results shown in Table 4 justify the assumption $\mu_M = \mu_V = \mu$. For each EP set, $\mu_M = \mu$ within 0.4%, although μ_V differs from μ by up to 25%. (They agree, by definition, at the baseline EP set.) The approximation $\mu_M = \mu_V = \mu$ is acceptably accurate due to the relatively small contribution of the shear term ($f_2 \cdot V/M \cdot h$) to MCF in comparison with that of the moment term (f_1). Over the 135 cases, the moment term (f_1) is always at least 8.7 times larger than the shear term ($f_2 \cdot V/M \cdot h$); ratios ≥ 20 are typical. Thus, any error in the prediction of MCF from using μ from Eq. (8) is negligible.

In Eqs. (3)–(6), F_1 and F_2 are dimensionless functions of notch and beam geometry. Upon determining μ, numerical values of F_1 and F_2 were computed for each geometry in the FE studies. Closed-form representations were derived to approximate F_1 and F_2 for any combination of D, R, L, h, and s within the range of the study. For application to diverse sizes of notched beams, notch geometry is conveniently expressed in terms of dimensionless variables. Several such nondimensional parameters were investigated. Numerous linear and nonlinear functions of the notch and beam dimensions (or nondimensional parameters) were fit to the 83 values of F_1 and F_2 resulting from the three FE studies. The relative performance of the various models was essentially constant across data sets—that is, the best models for F_1 and F_2 in the G8-E12 substudy (B) were also those most appropriate for the G32-E12 substudy (A) and the main study. F_1 and F_2 were fit well by the expressions:

$$F_1 = \frac{1}{0.165 - 0.217\phi + 0.145\delta} \tag{9}$$

$$F_2 = 1.23\phi^{0.67}\rho^{-0.55}\left(\frac{h}{3.5\text{ in.}}\right)^{0.164} \tag{10}$$

where $\phi \equiv D/h$, $\delta \equiv R/D$, and $\rho \equiv R/h$.

Both equations include dimensionless notch depth, ϕ, and a fillet radius term (ρ or δ). Beam span, s, does not appear since substudy A showed essentially no influence of s or span : depth ratio, s/h, on MCF. The notch length effect was negligible for $L \geq 1.5$ in., so L was dropped from the expressions.

Both substudies showed beam depth effects similar to those reported by Leicester (1969), Murphy (1986), Gustafsson (1988), and Masuda (1988)—that is, deep beams yielded higher stresses than did shallower ones with identical notch dimensions ϕ and R. Note that this effect is distinct from any probabilistic strength-size relationship, which is expected to be small for notched beams (Gustafsson 1988; Masuda 1988). The h effect on F_1 was described well by Eq. (9) without an explicit h term. This is because varying h changes the value of δ when ϕ and R are held constant. The δ term was found to account for both the R effect at h = constant and the h effect at R = constant. An explicit h term was needed to account for the beam depth effect on F_2. Since the beam depth exponent was not evaluated for the baseline EP set, Eq. (10) includes the exponent 0.164 derived from the G8-E12 substudy. The G32-E12 data yielded an exponent ≈ 0, i.e., a negligible beam depth effect on F_2. Thus, a beam depth exponent of 0.164 should give conservative results (high values of F_2 and MCF) for beams with $h \geq 3.5$ in. for all EP sets in this work.

Substituting Eqs. (3), (9), and (10) into Eq. (2) gives an algebraic expression that closely approximates the FE results:

$$\begin{aligned} \text{MCF} &\equiv \frac{\sigma_{h,\max}}{\left(\dfrac{6M}{th^2}\right)} \\ &= \mu\left[\frac{1}{0.165 - 0.217\phi + 0.145\delta} + \frac{V}{M}\cdot h\cdot 1.23\phi^{0.67}\rho^{-0.55}\left(\frac{h}{3.5\text{ in.}}\right)^{0.164}\right] \end{aligned} \tag{11}$$

Equation (11) fits the FE-computed MCF values very well. In the worst case, at the greatest notch depth ($\phi = 0.71$), Eq. (11) overpredicts MCF (i.e., is conservative) by about 13%. For the shortest notches, L = 1 in., the predictions are about 13% low (unconservative). Aside from these two extreme geometries, the simplified model provides estimates nearly indistinguishable from the actual MCF.

Mechanical test results

Two critical loads, recorded during the testing of each notched beam, were chosen for analysis using the CFHS model. These were load at crack initiation (P_i) and load immediately prior to the first significant drop ($\geq 2\%$) in load ($P_{2\%}$). The FE computations apply only

TABLE 4. *FE material constant μ defined in Eqs. (3)–(5).*

EP set[c]	μ (n = 135)[a]		μ_M (n = 15)[b]		μ_v (n = 15)[b]	
	Estimate	SE[d]	Estimate	SE[d]	Estimate	SE[d]
G8-E12	0.860	0.0010	0.862	0.0027	0.688	0.0080
G12-E12	0.911	0.0005	0.913	0.0013	0.785	0.0035
G17-E17	1.000	0	1.000	0	1.000	0
G22-E22	1.078	0.0006	1.076	0.0013	1.220	0.0083
G32-E12	1.154	0.0016	1.150	0.0045	1.442	0.0200

[a] n = Number of observations in the regression = (15 notch geometries)·(3 notch locations)·(3 loading conditions).
[b] n = Number of observations in the regression = 15 notch geometries.
[c] Elastic property set; see Table 2.
[d] Standard error of the estimate.

prior to crack initiation; the local geometry and stress distribution are altered greatly by the presence of a crack. For crack extension some small distance from the critical fillet, however, the resultant loading and notch depth (or net section) are about the same as for the uncracked fillet. Thus, the crack extension load in this region is roughly proportional to the crack initiation load, and the model is useful somewhat beyond crack initiation. Among the readily identified points on the load-displacement graph, $P_{2\%}$ was the highest load at which the model was generally useful. As expected, the ultimate load was quite variable and only modestly correlated with P_i.

Defining $\kappa_i \equiv \sigma_{h,i}/\mu$, Eq. (11) is rearranged:

$$\frac{6M_i}{th^2} = \frac{\kappa_i}{\left[\dfrac{1}{0.165 - 0.217\phi + 0.145\delta} + \dfrac{V}{M}\cdot h\cdot 1.23\phi^{0.67}\rho^{-0.55}\left(\dfrac{h}{3.5\ \text{in.}}\right)^{0.164}\right]} \tag{12}$$

where M_i is the resultant moment, at the critical fillet, at crack initiation.

Equation (12) can be rearranged and used to evaluate κ_i from notched beam test data, where M_i and V/M are known. Conversely, for known κ_i, Eq. (12) predicts moment capacity. The first ≥2% drop in load can be predicted by defining $M_{2\%}$ and $\kappa_{2\%}$, analogous to M_i and κ_i, respectively, and substituting them for M_i and κ_i in Eq. (12). Equation (12) can be written:

$$\frac{6M_{crit}}{th^2} = \kappa_{crit}g \tag{13}$$

where $g \equiv 1/(F_1 + F_2\cdot h\cdot V/M)$ and the subscript "crit" refers to either of the two critical loads. The quantity g reduces to a known constant for each test beam. A linear regression, with no intercept term, was performed to find the best value of κ for each material at each critical point. This technique also provided a measure of the significance of the predictive model.

The results of study 1 were analyzed first on the basis of $M^* \equiv 6M/th^2$ instead of κ, because $\delta = \rho = 0$ and L = 0.75 in. are not within the range of the simplified model and Eq. (12) may not be valid. Analyses of variance (ANOVA) showed that notch depth, D, was very highly significant ($P \leq 0.0001$) and accounted for ≥90% of the variability in M_i^* and $M_{2\%}^*$ for both oak and fir. The ANOVA models were all very highly significant ($P \leq 0.0001$). Conversely, all terms involving R or L were nonsignificant ($P \geq 0.05$). Based on the lack of difference between R = 0 and R = 0.25 in. results and the difficulty of notching beams with 0 < R < 0.25 in., no beams with radii <0.25 in. were included in the later experimental work. Results of the R = 0 tests and discussion of an extension of the CFHS model to treat unfilleted notches are given elsewhere (Zalph 1989).

Results from beams with R > 0 (study 2 and ~⅔ of study 1) were analyzed using Eq. (13) as well as regressions including a constant term to test the hypothesis of a non-zero intercept.

TABLE 5. *Regression results of Eq. (13) for studies 1 and 2 (R > 0).*

Material[a]	Critical load[b]	R_{max} = 0.5 in.[c]		Unadjusted[c]	
		κ, psi	SE[d]	κ, psi	SE[d]
Red oak (study A), dry	i	(all R < 0.5 in.)		27,160	1,860
(n = 16)[e]	2%			28,480	1,710
Fir (study A), dry	i	(all R < 0.5 in.)		13,570	616
(n = 17)	2%			14,620	527
Douglas-fir, dry	i	14,570	381	13,310	395
(n = 93)	2%	17,450	810	15,780	811
Spruce, dry	i	12,950	343	11,820	356
(n = 93)	2%	13,310	393	12,120	406
Southern yellow pine, dry	i	13,620	341	12,530	349
(n = 107)	2%	14,330	388	13,180	392
Southern yellow pine, green	i	13,160	342	12,120	341
(n = 106)	2%	14,160	437	13,030	430
Hard maple, green	i	21,360	373	19,560	416
(n = 93)	2%	21,350	376	19,540	424
Red oak, dry	i	18,800	392	17,260	392
(n = 93)	2%	19,380	411	17,770	421
Yellow-poplar, dry	i	17,970	311	16,490	333
(n = 94)	2%	18,400	366	16,930	356
Yellow-poplar, green	i	15,130	224	13,830	245
(n = 93)	2%	15,390	217	14,060	242

[a] From study 2, except as noted.
[b] i = at crack initiation; 2% = at first drop in load ≥2%.
[c] R_{max} = 0.5 in.: computed using R = 0.5 in. for any observations in which R > 0.5 in. Unadjusted: no substitution made. See text.
[d] SE: standard error of the parameter estimate.
[e] Number of specimens.

In all cases the model with no intercept was more highly significant, with much lower standard errors of κ. Each regression was highly significant ($P \leq 0.0001$). Regression results are given in Table 5. The high significance and low standard errors are evidence that the model correctly describes the general features of notched beam failure for all ten materials at both critical loads.

Table 5 includes two columns of κ results, calculated with and without the incorporation of an upper-limit fillet radius R_{max} into the calculation. R_{max} is the hypothetical fillet radius above which any increase in R no longer affects notched beam strength. Gerhardt (1984a) found that increasing R beyond 0.5 in. (with h = 3.75 in.) resulted in no increase in beam strength, despite FE results to the contrary. To set R_{max} = 0.5 in., F_1 and F_2 were calculated using δ and ρ corresponding to R = 0.5 in. whenever R ≥ 0.5 in. occurred in the experimental data. The regressions were more significant (higher F-statistics) and had slightly lower standard errors of κ when computed using R_{max} = 0.5 in. We concluded that R_{max} = 0.5 in. is appropriate for all of the materials tested.

Figure 2 shows the predicted versus actual crack initiation loads (P_i) for the eight species tested in study 2. The predictions are based on the κ values computed using R_{max} = 0.5 in. The plot demonstrates the goodness of fit indicated by the very high significance and low standard errors of the Eq. (13) regression results (Table 5). Similar results were obtained by plotting predicted versus actual $P_{2\%}$ values, with only slightly more scatter about the line of equality. The regression residuals were not systematically related to any of the geometric variables (ϕ, δ, ρ, and V/M). We conclude that the theoretically derived term, g, closely approximates the geometry dependence of notched

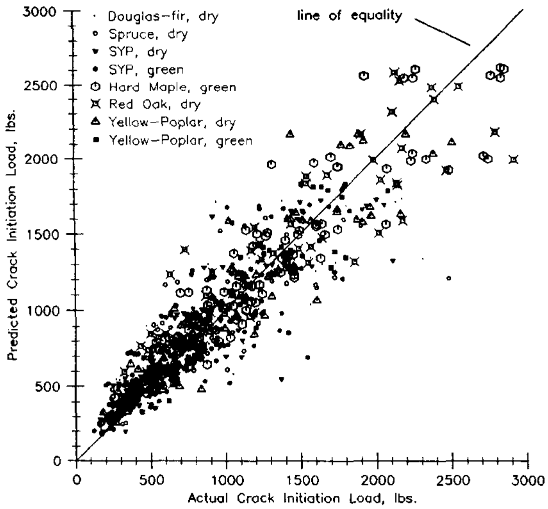

FIG. 2. Predicted versus actual crack initiation loads, study 2. Eight species. $R_{max} = 0.5$ in.

beam failure loads, and that κ is essentially geometry independent. This is a key validation of the model.

Results of the unnotched bending and small, clear specimen tests are summarized in Table 6. Linear models were constructed relating group mean κ_i and $\kappa_{2\%}$ to the group means of S, $T_\perp$, MOR, and G. Since eight materials were tested, each regression model had eight total degrees of freedom. The best models were:

$$\kappa_i = 12.4 \cdot T_\perp + 19{,}370 \cdot G \qquad (14)$$

and

$$\kappa_{2\%} = 8.94 \cdot T_\perp + 23{,}890 \cdot G \qquad (15)$$

with no intercept terms. (κ and $T_\perp$ are given in psi.) Each model was very highly significant ($P \leq 0.0001$). $T_\perp$ and G were found to be essentially independent, with $r^2 = 0.33$ and no discernible relationship on an x-y plot. The strong relationship between κ and the material properties $T_\perp$ and G is clear evidence that κ is essentially a material constant.

SUMMARY OF PRINCIPAL FINDINGS

A simplified model of notched beam strength, Eq. (12), gives good predictions of critical loads. Crack initiation load is predicted particularly well. Ultimate load was found to be the most variable and least well-described by the model. The first major drop in load (i.e., $P_{2\%}$) may be used as a conservative estimate of ultimate capacity.

Predicting notched beam failure loads using a geometry factor and a material factor was validated. This formulation is applicable to hardwoods and softwoods over a wide range of density and properties. The material parameter, κ, used in the model is estimated well by a linear combination of perpendicular-to-grain tensile strength and density. This allows strength predictions to be made for species for which κ has not been determined directly. Like all wood properties, κ is variable. Reliability-based design procedures or safety factors must be used to account for this variability in structural design and evaluation.

Notch fillet radius affects beam strength for

TABLE 6. *Results of unnotched bending and small, clear specimen tests. n = 30 except as noted.*

Material	Shear (psi)	$T_\perp$[a] (psi)	G[b] (g/cm³)	MOR[c] (psi)	κ_i[d] (psi)	$\kappa_{2\%}$[d] (psi)
Douglas-fir, dry	1,755	360	0.55	12,780	14,570	17,450
Spruce, dry	990	301	0.44	7,670	12,950	13,310
SYP, dry	1,255	358	0.50	7,960	13,620	14,330
SYP, green	835	287	0.51	6,300	13,160	14,160
Maple, green	1,440	575	0.63	7,420	21,360	21,350
Red oak, dry	2,260	673	0.63	12,810	18,800	19,380
Yellow-poplar, dry	1,780	655	0.49	10,630	17,970	18,400
Yellow-poplar, green	890	472	0.47	6,230	15,130	15,390

[a] Perpendicular-to-grain tensile strength.
[b] Dry-basis density.
[c] Modulus of rupture.
[d] κ_i and $\kappa_{2\%}$ calculated using $R_{max} = 0.50$ in. (Table 5); n = 93.

$R \leq 0.5$ in., above which strength remains essentially constant.

The CFHS approach is uniquely general in its applicability. It is the only closed-form method available for treating the effects of fillet radius and beam depth in addition to those of notch depth and loading condition. Its single material parameter, κ, can be determined from a relatively simple mechanical test or can be estimated from existing values of density and cross-grain tensile strength. The predictive equation has the attributes of simplicity, accuracy, and generality necessary for wide use as in designing and evaluating interior-notched wood beams.

ACKNOWLEDGMENTS

The authors thank Dr. Terry Gerhardt, Sonoco Products Company, and Mr. Greg Foliente, VPI&SU, for their help with this study. This work was funded by a grant from the USDA Forest and Rangeland Renewable Resources Competitive Grants program.

REFERENCES

Abou-Ghaida, S., and V. K. A. Gopu. 1984. Shear strength of notched timber beams. Proc. Pacific Timber Engin. Conf., Auckland, NZ, May 21–25, 1984.

American Society for Testing and Materials. 1986. Standard methods of testing small clear specimens of timber. ASTM D143-83, Philadelphia, PA.

Anderson, L. O. 1975. Wood frame house construction. Agriculture Handbook No. 73, USDA Forest Service.

Barrett, J. D. 1974. Effect of size on tension perpendicular-to-grain strength of Douglas-fir. Wood Fiber 6(2): 126–143.

Bendtsen, B. A., and S. Porter. 1978. Comparison of results from standard 2-inch with 1½-inch shear block tests. Forest Prod. J. 28(7):54–56.

Byars, E. F., and R. D. Snyder. 1975. Engineering mechanics of deformable bodies, 3rd ed. 499 pp. Intext Educational Publishers, New York. Pp. 216–224.

Canadian Forestry Service. 1976. Reusable wood pallets: Selection and proper design. Forestry Technical Rept. 11. Can. For. Serv. Eastern For. Prod. Lab., Ottawa, Ont, Canada.

Gerhardt, T. D. 1983. Plane stress analysis of wood members using isoparametric finite elements. USDA For. Serv. Gen. Tech. Rept. FPL 35. For. Prod. Lab., Madison, WI.

———. 1984a. Strength and stiffness analysis of notched, green oak pallet stringers. Res. Paper FPL 452. USDA For. Serv. For. Prod. Lab., Madison, WI.

———. 1984b. A hybrid/finite element approach for stress analysis of notched anisotropic materials. ASME J. Appl. Mechanics 51:804–810.

Green, A. E. 1942. Stress systems in aeolotropic plates, IV. Proc. Roy. Soc. London A 180:173–208.

———, and G. I. Taylor. 1945. Stress systems in aeolotropic plates, III. Proc. Roy. Soc. London A 184:181–195.

Gustafsson, P. J. 1988. A study of strength of notched beams. Paper CIB-W18A/21-10-1. Intl. Council for Bldg. Res. Studies and Documentation, Vancouver, B.C., Canada.

Leicester, R. H. 1969. The size effect of notches. Proc. 2nd Australasian Conf. on Mech. of Structures and Materials. V4:1–20.

———, and W. G. Poynter. 1979. On the design strength of notched beams. *In* Proc. of the 19th Forest Products Research Conference, Melbourne, Australia.

Mall, S., J. F. Murphy, and J. E. Shottafer. 1983. Criterion for mixed mode fracture in wood. ASCE J. Engin. Mechanics 109(3):680–690.

Masuda, M. 1988. Theoretical consideration on fracture criteria of wood—Proposal of finite small area theory. Pages 584–595 *in* Proc. of the 1988 Intl. Conf. on Timber Engineering, Seattle, WA, 1988. For. Prods. Res. Soc., Madison, WI.

Murphy, J. F. 1979. Using fracture mechanics to predict failure in notched wood beams. Pages 159–173 *in* Proc. of the 1st Intl. Conf. on Wood Fracture, Banff, Alberta, 1979. Forintek Canada Corp., Vancouver, B.C., Canada.

———. 1986. Strength and stiffness reduction of large notched beams. J. Struct. Engin. 112(9):1989–2000.

Myers, R. H. 1971. Response surface methodology. Allyn and Bacon, Publ., Boston, MA. 246 pp.

Porter, A. W. 1964. On the mechanics of fracture in wood. Forest Prod. J. 14(8):325–331.

Standards Assoc. of Australia. 1988. SAA timber structures code. Part 1—Design methods. AS 1720.1-1988. SAA, North Sydney, N.S.W.

Stern, E. G. 1990. Personal communication. Professor Emeritus, Dept. of Wood Science and Forest Products, Virginia Polytechnic Institute and State University.

Stieda, C. K. A. 1964. Stress concentrations in notched timber beams. Trans. Engin. Inst. of Canada, vol. 7, No. A-5. Paper No. EIC-64-BR & STR 5. 6 pp.

———. 1966. Stress concentrations around holes and notches and their effect on the strength of wood beams. J. Materials 1(3):560–582.

USDA Forest Products Laboratory. 1987. Wood handbook: Wood as an engineering material. Hdbk. No. 72. USDA For. Prod. Lab., Madison, WI.

Zalph, B. L. 1989. Predicting the strength of notched wood beams. Doctoral dissertation, Virginia Polytechnic Inst. and State Univ., Blacksburg, VA.